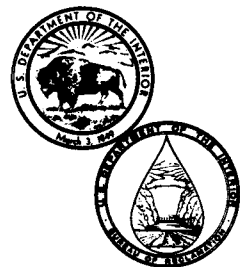


HYDRAULIC MODEL STUDIES ON BULB TURBINE INTAKES

March 1983

Engineering and Research Center

**U.S. Department of the Interior
Bureau of Reclamation**



1. REPORT NO. REC-ERC-82-14	2. GOVERNMENT ACCESSION NO.	3. RECIPIENT'S CATALOG NO.
4. TITLE AND SUBTITLE Hydraulic Model Studies on Bulb Turbine Intakes	5. REPORT DATE March 1983	6. PERFORMING ORGANIZATION CODE
	8. PERFORMING ORGANIZATION REPORT NO. REC-ERC-82-14	
7. AUTHOR(S) Clifford A. Pugh	10. WORK UNIT NO.	11. CONTRACT OR GRANT NO.
9. PERFORMING ORGANIZATION NAME AND ADDRESS Bureau of Reclamation Engineering and Research Center Denver, Colorado 80225	13. TYPE OF REPORT AND PERIOD COVERED Bureau of Reclamation Denver, Colorado	14. SPONSORING AGENCY CODE DIBR
		12. SPONSORING AGENCY NAME AND ADDRESS Same
15. SUPPLEMENTARY NOTES Microfiche and/or hard copy available at the Engineering and Research Center, Denver, CO Ed:BDM		
16. ABSTRACT <p>Intakes for bulb and rim generator turbines are very large in relation to their runner diameters. Because the water velocity is low in the intake area, the losses are small. This report describes research on the effect that simplifying the intake design has on energy losses and flow distribution. Using straight surfaces in place of curved bellmouth entrances and shortening the length of the intake could significantly reduce construction costs. In addition, reducing the intake size would reduce the size of trashracks, gates, and associated operating equipment.</p>		
17. KEY WORDS AND DOCUMENT ANALYSIS a. DESCRIPTORS-- hydraulic models/ air models/ *intakes/ low head/ hydroelectric powerplants/ *bulb turbines/ flow passages/ energy losses/ *head losses/ pressure head/ velocity distribution/ cost savings b. IDENTIFIERS-- rim generator turbine intakes/ *bulb turbine intakes/ value engineering c. COSATI Field/Group 13G COWRR: 1307.1 SRIM: 97C		
18. DISTRIBUTION STATEMENT <i>Available from the National Technical Information Service, Operations Division, 5285 Port Royal Road, Springfield, Virginia 22161.</i> (Microfiche and/or hard copy available from NTIS)	19. SECURITY CLASS (THIS REPORT) UNCLASSIFIED	21. NO. OF PAGES 18
	20. SECURITY CLASS (THIS PAGE) UNCLASSIFIED	22. PRICE

REC-ERC-82-14

**HYDRAULIC MODEL STUDIES
ON BULB TURBINE INTAKES**

by
Clifford A. Pugh

March 1983

**Hydraulics Branch
Division of Research
Engineering and Research Center
Denver, Colorado**



UNITED STATES DEPARTMENT OF THE INTERIOR

*

BUREAU OF RECLAMATION

ACKNOWLEDGMENTS

Research was performed in the Hydraulic Laboratory of the Bureau of Reclamation's Engineering and Research Center. The study was sponsored by the Department of Energy under agreement EG-77-A-36-1024 with the Bureau of Reclamation.

Dr. H.T. Falvey and T.J. Rhone provided valuable technical review and comments during the course of the study. Richard Phillips, Robert McGovern, and Cheryl States were instrumental in accomplishing the testing and data analysis.

As the Nation's principal conservation agency, the Department of the Interior has responsibility for most of our nationally owned public lands and natural resources. This includes fostering the wisest use of our land and water resources, protecting our fish and wildlife, preserving the environmental and cultural values of our national parks and historical places, and providing for the enjoyment of life through outdoor recreation. The Department assesses our energy and mineral resources and works to assure that their development is in the best interests of all our people. The Department also has a major responsibility for American Indian reservation communities and for people who live in Island Territories under U.S. Administration.

CONTENTS

	Page
Glossary	iv
Purpose	1
Introduction	1
Conclusions	1
Scope of study	1
Model design and similarity	1
The model	2
Test procedures and instrumentation	3
Discharge measurement	3
Velocity measurement	7
Pressure measurement	7
Results	8
Velocities	8
Pressures	8
Euler number accuracy	8
Overall losses through the model	8
Example calculation of relative losses	10
Pressure drop coefficients	10
Additional testing	12
Pressure drop along intake surfaces	13
Intake pressure data accuracy	13
Wicket gate angle vs. percent gate opening	13
Bibliography	18

TABLES

1 Pressure drop through the model	11
2 Comparison of intake losses	11

FIGURES

1 Euler number vs. Reynolds number	2
2 Schematic diagram of the test apparatus	2
3 Overall view of test apparatus	3
4 Bulb turbine model	4
5 The four intakes tested	5
6 Closeup views of the model	6
7 Velocity measurement with hot-wire anemometer	7
8 Pressure measurement system	7
9 Pressure transducer calibration curve	8
10 Velocity distributions for the four intakes ($\theta = 30^\circ$)	9

CONTENTS

FIGURES—Continued

		Page
11	Velocity profiles along data column 3 in figure 10	10
12	Pressure drop through the model—comparison of four intakes	12
13	Intake 1 with a center pier	13
14	Pressure drop through the model—intake 1, with and without a bulkhead slot	14
15	Pressure drop through the model—intake 1, with and without a center pier in the intake	14
16	Pressure drop through the model—intake 1, approach channel comparison	14
17	Pressure drop through the model—intake 1, with and without a draft tube	14
18	Pressure drop along intake surfaces—intake 1	15
19	Pressure drop along intake surfaces—intake 2	15
20	Pressure drop along intake surfaces—intake 3	15
21	Pressure drop along intake surfaces—intake 4	15
22	Pressure drop comparison, top centerline—four intakes	16
23	Pressure drop comparison, left side centerline—four intakes	16
24	Pressure drop comparison, right side centerline—four intakes	16
25	Pressure drop comparison, bottom centerline—four intakes	16
26	Pressure fluctuations, intake 1, top centerline	17
27	Pressure drop comparison, intake 1, data repeatability	17
28	Percent gate opening vs. wicket gate angle	17

GLOSSARY

<p>A_r = flow area at the runner</p> <p>C_p = pressure drop coefficient</p> <p>C = coefficient of discharge</p> <p>d = diameter</p> <p>D = reference length</p> <p>d/D = relative depth in intake</p> <p>$D1$ = runner diameter</p> <p>E = Euler number</p> <p>E' = Velocity of approach factor</p> <p>g = acceleration due to gravity</p> <p>Δh = relative loss</p> <p>H = gross head</p> <p>h_w = pressure drop across orifice</p> <p>K = flow coefficient</p> <p>$L/D1$ = reference distance</p> <p>p, p_1, p_2 = pressures</p> <p>Δp = pressure drop</p>	<p>P_1 = Inlet pressure</p> <p>Q = flow rate, or discharge</p> <p>R = Reynolds number</p> <p>T_1 = ambient temperature</p> <p>V = velocity</p> <p>V_i = average intake velocity in the axial direction</p> <p>V_r = average velocity at the runner in the axial direction</p> <p>\bar{V} = average velocity</p> <p>Y = adiabatic expansion factor</p> <p>β = diameter of orifice/diameter of pipe</p> <p>γ = specific force = ρg</p> <p>γ_a = specific force of air</p> <p>θ = wicket gate angle</p> <p>ν = kinematic viscosity</p> <p>ρ = density</p>
---	--

PURPOSE

The purpose of this study was to investigate possible simplifications in the design of the intake flow passages for bulb turbines and to determine the head losses associated with these simplifications. Simplifying the design and construction of bulb turbine intakes could lead to cost savings in both material and labor.

INTRODUCTION

The main obstacle in the development of small hydroelectric powerplants has been economics; in most cases, the cost per installed kilowatt for small hydropower is still higher than for fossil fuel plants. For low-head hydroelectric installations, with head less than 20 m, the major costs are the initial investment in the civil works structure and the fluid machinery. If the cost of the structure can be reduced without introducing additional head losses, more small hydroelectric installations would be feasible.

Intakes for bulb and rim generator turbines are very large in relation to their runner diameters. Because the water velocity is low in the intake section, the losses are small. It was concluded in an earlier literature review [1]¹ that savings could be achieved by replacing curved surfaces with straight surfaces and shortening the length of the intake. Reducing the intake size would result in additional savings in trashracks, bulkheads, entrances, gates, and the associated operating equipment.

Another small-hydropower reference [2] states that "Irregularities of flow as well as flow separations in the intake section have an unfavorable effect on the turbine's hydraulic behavior, and an optimum design for the intake portion is therefore essential for smooth, undisturbed turbine performance." However, the data presented herein demonstrate that simplifications in the intake section do not adversely affect the flow field leading to the guide vanes and runner.

CONCLUSIONS

- Significant simplifications and size reductions can be made in the intakes of bulb and rim generator turbines without increasing energy losses or adversely affecting flow distribution.

¹Numbers in brackets refer to entries in the bibliography.

- Comparative energy losses and velocity distributions illustrate the advantages of using simplified intake designs.
- Structural costs for a bulb turbine structure using a simplified intake design (intake 4) would be about 10 percent less than the present standard design (intake 1).

SCOPE OF STUDY

A model of a typical bulb turbine installation was built in such a manner that the intake section could be readily removed to permit comparison of other intake shapes with the conventional shape. The model dimensions basically corresponded to standard flow passage dimensions used by a major manufacturer. After testing the original intake, three other intakes of various shapes and sizes were tested and the results compared. Dimensions are given in terms of the runner diameter, D_1 .

Extensive testing was done on the original intake to determine the effect of a bulkhead slot, a pier in the intake, a draft tube, and various approach channel configurations.

MODEL DESIGN AND SIMILARITY

An air model was used in this study. Advantages of an air model over a water model include: (1) flexible, easy model construction, (2) little problem of leakage, and (3) quick model measurements and changes. The disadvantages are: (1) small levels of pressure differences, requiring delicate measuring apparatus; and (2) inability to simulate a free surface. Air models can be used to study hydraulic problems in which the flow is governed by inertia and viscosity effects [3]. Conditions of flow at an entry and flow through pressurized conduits fall within this category. The criterion of similarity for this type of flow and for transferring results to prototype conditions is well known to be the Reynolds model law (equation 1).

$$\text{Reynolds number} = R = \frac{VD}{\nu} \quad (1)$$

where:

V = velocity

D = a characteristic length

ν = kinematic viscosity

Most prototype hydraulic structures have Reynolds numbers of the order of magnitude of 10^6 to 10^8 . The achievement of these Reynolds numbers under laboratory conditions would require blowers with enormous capacity. It is possible, however, to attain approximate similarity at Reynolds numbers of about 10^4 to 10^5 . At these Reynolds numbers, viscosity has little effect. It is also necessary to build the model large enough to avoid undesirable compressibility effects [3]. The model was designed to keep the Reynolds number as high as possible while limiting the air velocity to less than 50 m/s to avoid compressibility effects.

The Euler number is a dimensionless ratio which relates inertia forces to pressure forces (equation 2).

$$\text{Euler number} = E = \frac{\rho V^2}{\Delta p} \quad (2)$$

where:

- ρ = fluid density
- Δp = pressure drop
- V = velocity

In incompressible fluids and in the absence of other forces (such as viscosity and gravity), the Euler number is exclusively a function of the geometry of the flow boundaries [3]. At Reynolds numbers high enough to attain similarity, the Euler number is a constant. Therefore, the Euler number will be the same for any prototype size as it is in the model if the geometry is similar. For this reason, the Euler number is also referred to as the geometrical flow number [3].

The first set of tests was conducted to determine the minimum discharge to obtain similarity. Tests were run at different discharges for the same model configuration. At Reynolds numbers greater than 10^5 , the Euler number is approximately constant (fig. 1). Therefore, all of the tests were conducted at Reynolds numbers greater than 10^5 . The Euler number is then used to scale results from the model to prototype conditions.

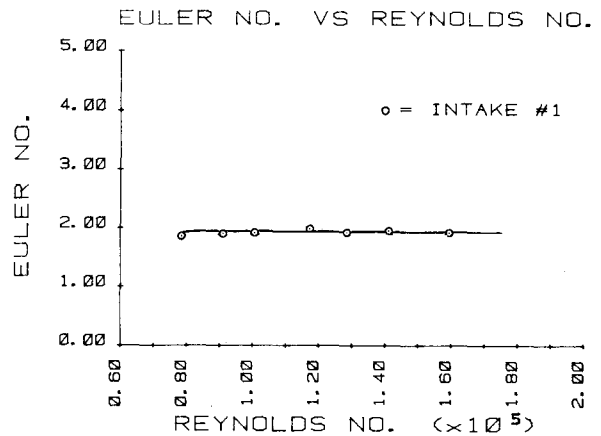


Figure 1.—Euler number vs. Reynolds number.

THE MODEL

Figure 2 is a schematic diagram of the test apparatus and figure 3 shows an overall view of the apparatus itself. Air was supplied by a blower through a supply line and orifice plate to a stilling chamber (plenum), where it entered the model intake section.

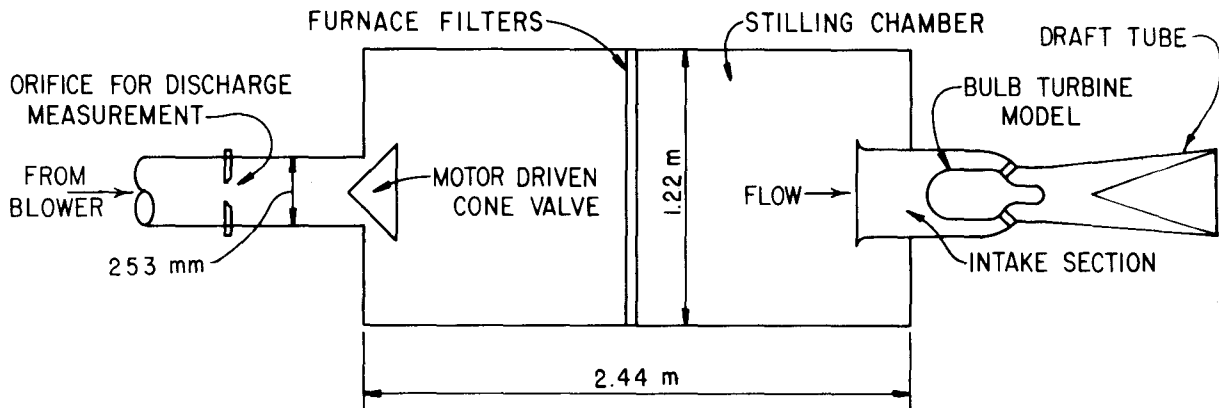


Figure 2.—Schematic diagram of the test apparatus.

Figure 4 shows the configuration of the bulb turbine model with the conventional intake section (intake 1). All four intake designs used in this study are shown on figure 5. The intake sections were made of sheet metal, and piezometer taps were included along the top, bottom, and sides of each intake to measure the pressure drop along these surfaces (fig. 5). A pressure tap was also included in the plenum to measure the total pressure required to produce a given flow through the model.

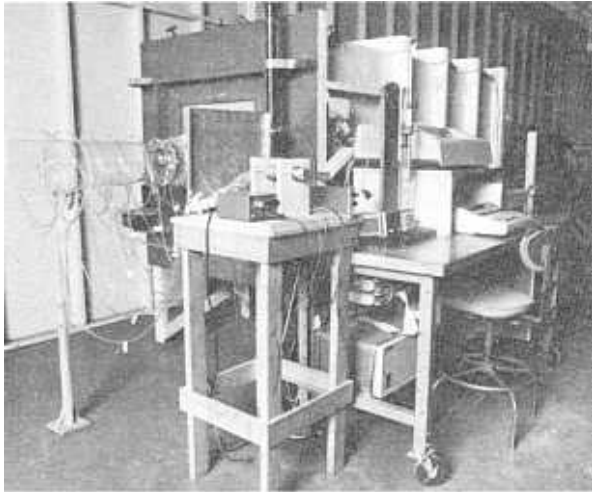


Figure 3.—Overall view of test apparatus. P801-D-79881

The flow passage downstream from the intake section, including the draft tube, was made of transparent plastic. The wicket gates and bulb were formed from wood, and the piers supporting the bulb were made of high density polyurethane. Figure 6 shows closeup views of various parts of the model.

The wicket gates were operated simultaneously with a control ring. Figure 4 contains a definition sketch for the wicket gate opening angle, θ . This angle was adjustable from 0° to 60° , with 0° being full open. Runner blades were not included in the model because the focus of the study was the effect of changes in the intake flow passage geometry. The changes in Euler number due to changes in flow passage geometry are not affected by the runner blades.

TEST PROCEDURES AND INSTRUMENTATION

Data collected during the tests included: (1) total discharge through the model; (2) velocity profiles

immediately upstream from the bulb (at the bulk-head slot in fig. 4); (3) pressures along the top, bottom, and sides of the intake; and (4) plenum and atmospheric pressures.

Discharge Measurement

The rate of flow, or discharge, was measured with a concentric, thin-plate orifice located in the supply line (figs. 2 and 6). Flange taps just upstream and downstream from the orifice plate were used to obtain the pressure differential across the plate.

Equations for computing actual rates of flow through an orifice plate are found in *Fluid Meters, Their Theory and Application* [4]. Flow rate, Q , was computed as follows:

$$Q = 18.794 KYd^2 \sqrt{h_w \frac{T_1}{P_1}} \quad (3)$$

where:

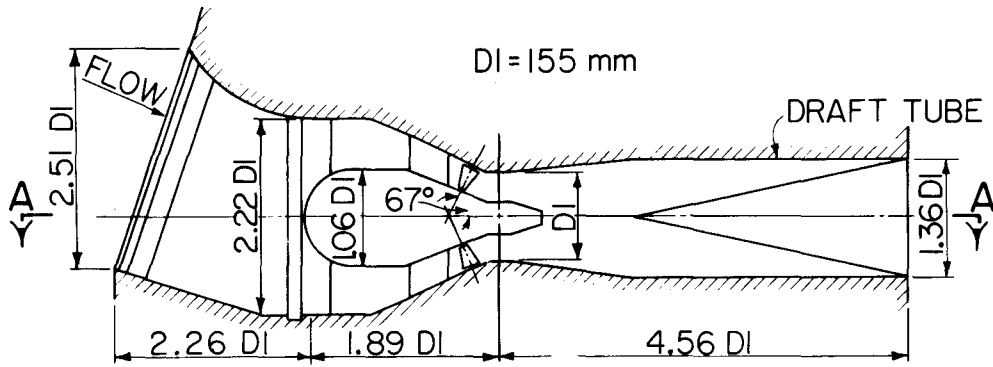
- Q = flow rate (m^3/s)
- Y = adiabatic expansion factor
- h_w = pressure drop across orifice (kPa)
- d = diameter of orifice (m)
- P_1 = inlet pressure (kPa – absolute)
- T_1 = temperature (kelvins)
- K = flow coefficient = CE'
- C = coefficient of discharge
- β = diameter of orifice/diameter of pipe
- E' = velocity of approach factor = $\frac{1}{\sqrt{1 - \beta^4}}$

For $K = 0.622$ (from equation I-5-76 in [4]), $d = 0.1222$ m, $Y = 0.991$ (from equation I-5-50 in [4]), and $\beta = 0.483$, equation 3 can be approximated by:

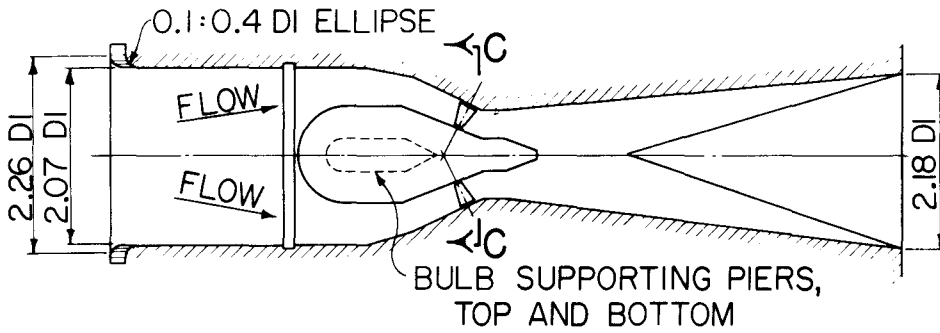
$$Q = 0.1730 \sqrt{h_w \frac{T_1}{P_1}} \quad (4)$$

The following procedure was used for each test:

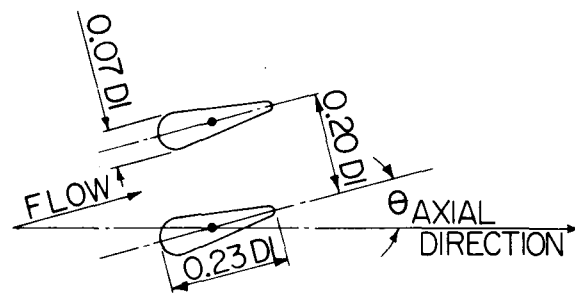
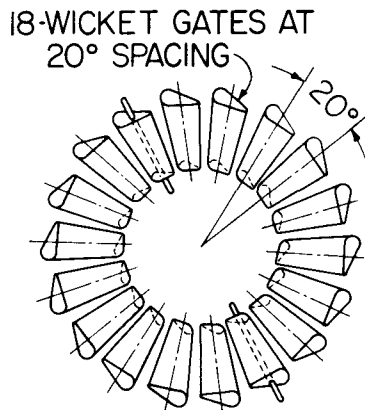
1. Record the barometric pressure
2. Record the ambient temperature, T_1



SECTION THROUGH BULB TURBINE MODEL



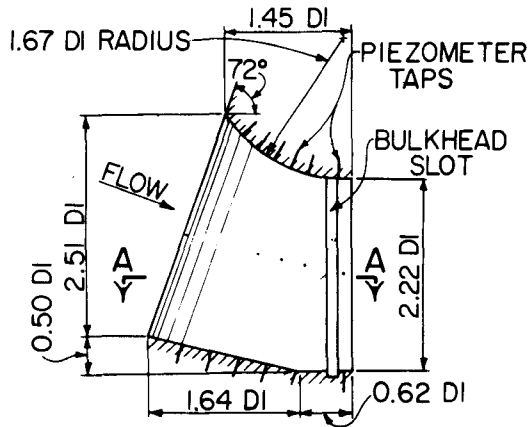
SECTION A-A



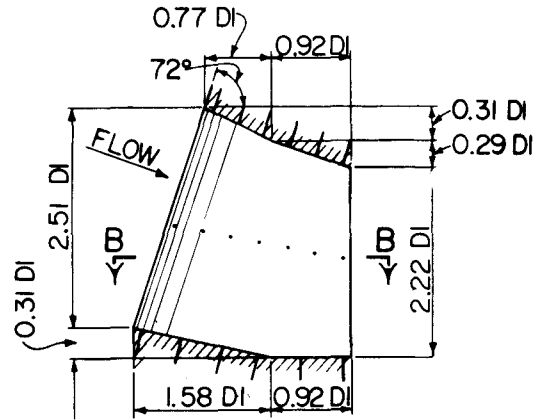
WICKET GATE OPENING DETAIL

SECTION C-C

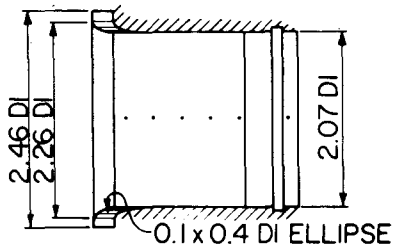
Figure 4.—Bulb turbine model (with intake 1 shown).



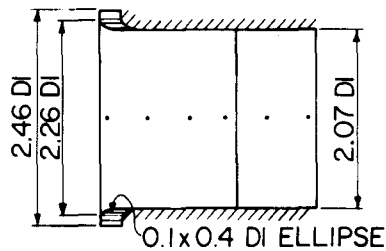
SECTION THROUGH INTAKE NO. 1



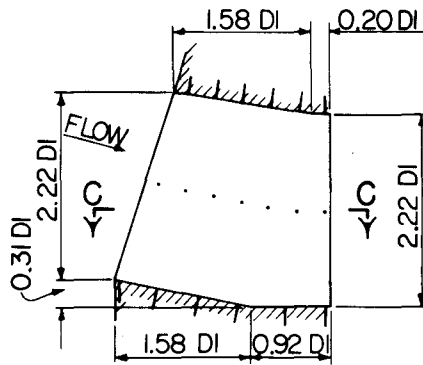
SECTION THROUGH INTAKE NO. 2



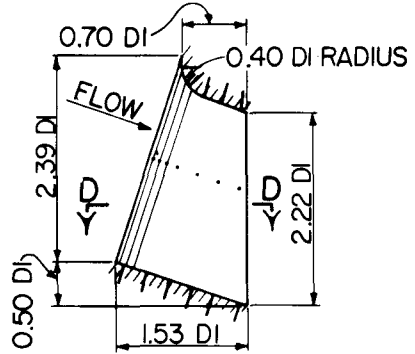
SECTION A-A



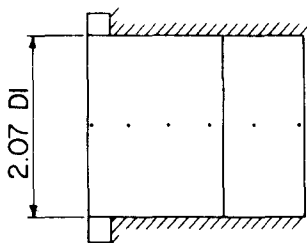
SECTION B-B



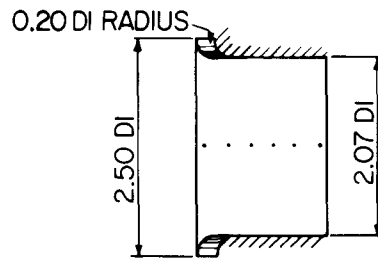
SECTION THROUGH INTAKE NO. 3



SECTION THROUGH INTAKE NO. 4

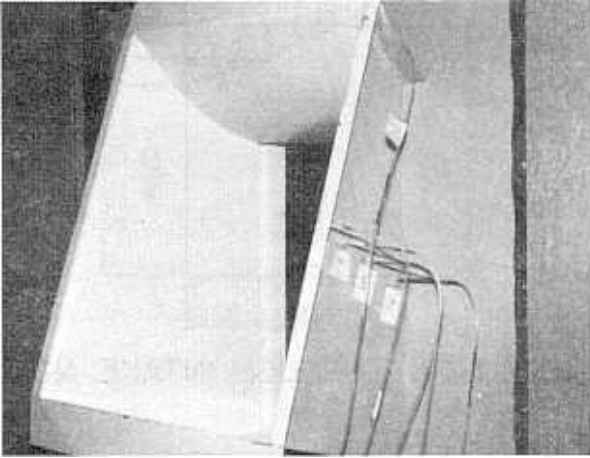


SECTION C-C

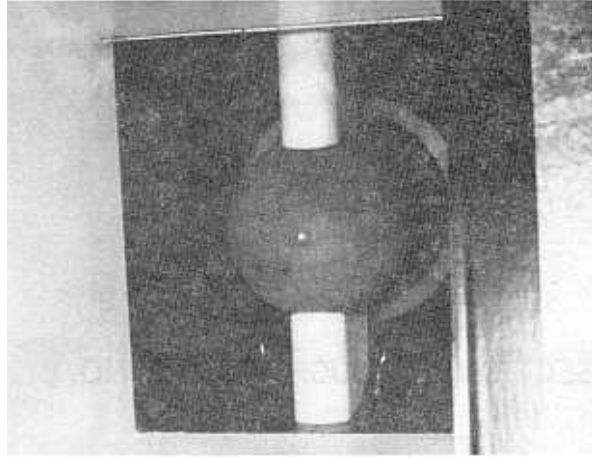


SECTION D-D

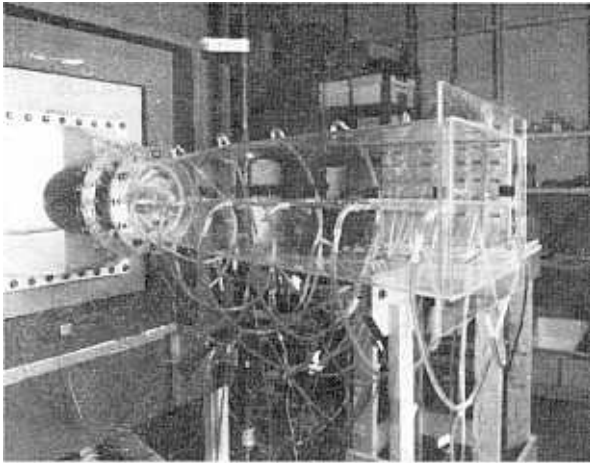
Figure 5.—The four intakes tested. (D1=runner diameter=155 mm)



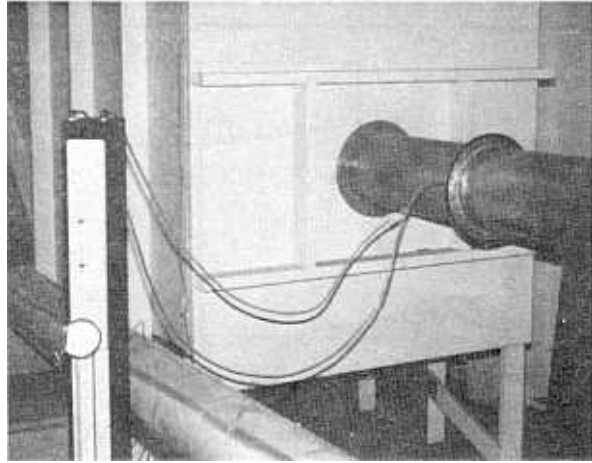
(a) Intake 1 without approach channel (looking downstream from inside plenum). P801-D-79882



(b) Bulb, piers, and wicket gates (looking downstream through intake). P801-D-79883



(c) Bulb turbine and draft tube (looking upstream). P808-D-79884



(d) Supply pipe with orifice plate (looking downstream). P801-D-79885

Figure 6.—Closeup views of the model.

3. Record the inlet pressure, P_1
4. Record differential pressure across the orifice plate, h_w
5. Compute the flow rate, Q
6. Record velocity or pressure data

Velocity Measurement

Velocity measurements were made for each intake at various wicket gate openings. Measurements were made at the bulkhead slot location immediately upstream from the bulb (fig. 5) using a hot-wire, constant-temperature anemometer (fig. 7). For each test, 117 velocity measurements were taken in a 9- by 13-point grid using a telescoping probe attached to the self-contained instrument, and the readings were recorded manually. The hot-wire anemometer readings were checked by measuring known velocities through an orifice in the side of the stilling chamber.

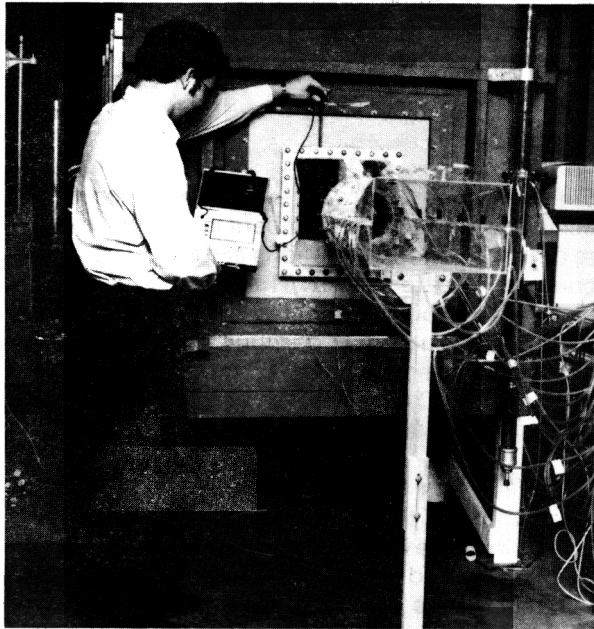


Figure 7.—Velocity measurement with hot-wire anemometer. P801-D-79886

Pressure Measurement

Pressure differences in an air model are small. Therefore, sensitive and accurate instruments are needed to collect acceptable data.

Pressure taps from the orifice plate, the intake, and the plenum were all connected to a single

scanning-type pressure sampling valve for measuring multiple pressures. With this system, one pressure transducer was used to measure all the pressures. A manually operated step drive was used to connect each pressure line sequentially to a center port in the valve (fig. 8), and the center port was connected to a ± 6.895 -kPa differential pressure transducer having a total error of 0.06 percent (combined linearity and hysteresis). The opposing side of the transducer was open to atmospheric pressure. Calibration pressures were applied to the transducer with a known height water column. Figure 9 shows the calibration curve. The lack of scatter in the data around the calibration curve demonstrates the accuracy of the transducer.

Transducer excitation was 12 V d.c., and the output was amplified 1000 times with a high-gain data amplifier. The amplified output was in the range of -5 to $+8$ volts. Output voltages, read with a high speed DVM (digital voltmeter), were collected and stored using a data acquisition system. A microprocessor (fig. 3) was programmed to read average and fluctuating voltages from the DVM. The voltages were converted to pressures and, when the test was complete, the data were transferred from memory to cassette tape for later printing, plotting, and analysis. Atmospheric pressure was recorded before and after each test to ensure that the reference pressure did not vary substantially during the test.

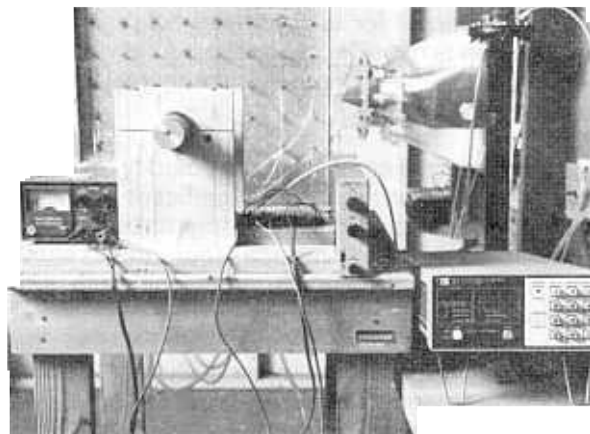


Figure 8.—Pressure measurement system. Left to right are the power supply, scanning-type pressure sampling valve (pressure transducer is inside the valve), terminal strip, high gain amplifier, and digital voltmeter. P801-D-79887

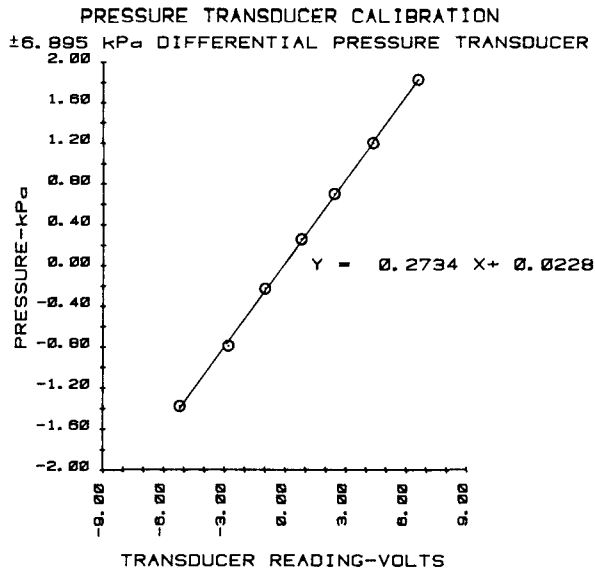


Figure 9.—Pressure transducer calibration curve.

RESULTS

Velocities

Velocity distributions for a given intake design were very similar when the wicket gate angles (θ) were less than 45° . For 45° and 60° wicket gate angles, the profiles were very erratic and unsymmetrical.

Velocity distributions were plotted for the four intakes for $\theta = 30^\circ$ (fig. 10). The average velocity, \bar{V} , was different for each intake; however, flow distribution is not affected by the actual values of velocity if the Euler number is constant. (See the section on similarity.)

It is obvious from comparing the velocity contours that the intake shape has a significant effect on velocity distribution. (See fig. 5 for intake shapes.) The velocity distributions for all four intakes show the flow stagnating in front of the bulb and flowing around it to the sides.

In intake 1, the velocities were high near the top, due to the smooth, bellmouth-type top curve, and low near the bottom, with a steep transition from top to bottom.

In intake 2, the velocities were fairly uniform throughout, and the local velocities did not vary greatly from the average velocity.

Intake 3 did not have entrance curves and the corners were square. The effect of the square corners is apparent in the velocity profiles. Velocities were high through the center portion of the profile and very low at the edges and corners.

Flow distribution in intake 4 was fairly uniform. The pattern did not indicate separation as in intake 3, nor a steep gradient from top to bottom as in intake 1. The overall velocity distribution was the most uniform in intake 4.

Velocity profiles from top to bottom along data column 3 in figure 10 are plotted in figure 11. This graph illustrates the differences in flow distribution among the four intakes in the zone where most of the flow passes around the bulb.

It should be noted that the average velocity head, $\bar{V}^2/2g$, in the intake section is usually only about 1 percent of the total prototype head. Therefore, flow irregularities in the intake section should have relatively minor effect on losses through the structure.

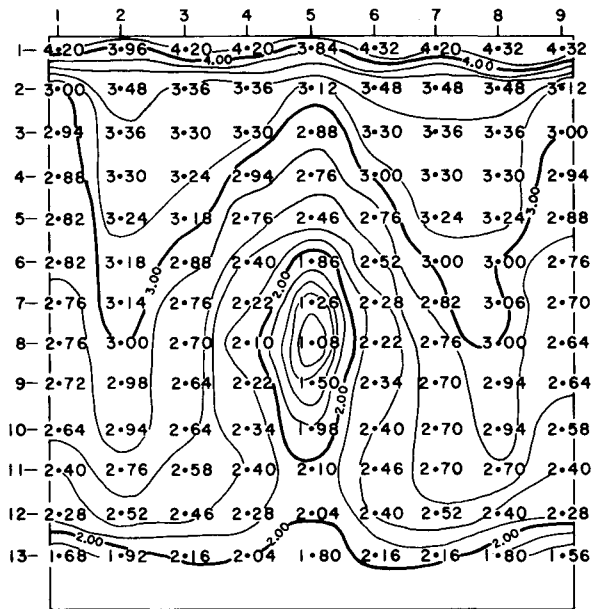
Pressures

Euler number accuracy. — An indication of the accuracy of the Euler numbers is needed in order to determine if the variations are due to geometry changes or data scatter. Therefore, several runs were made for the same geometry at different discharges (runs 101 through 116). The Euler numbers varied by ± 0.015 ; therefore, changes greater than 0.015 are due to geometry effects rather than data scatter.

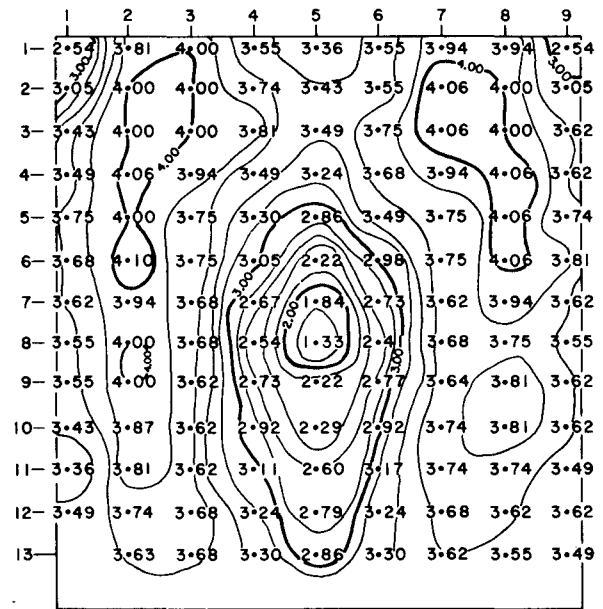
Overall losses through the model. — Pressure drops through the entire model as well as pressures along the flow surfaces in the intake section were measured for each test run. Table 1 lists the Euler numbers for the different configurations tested. These data can be used to assess the effect of changes in geometry on pressure drops (losses) through the model. The table also defines the model configuration for each run number.

The reference velocity used to calculate the Euler numbers in table 1 was the average axial velocity at the runner, \bar{V}_r .

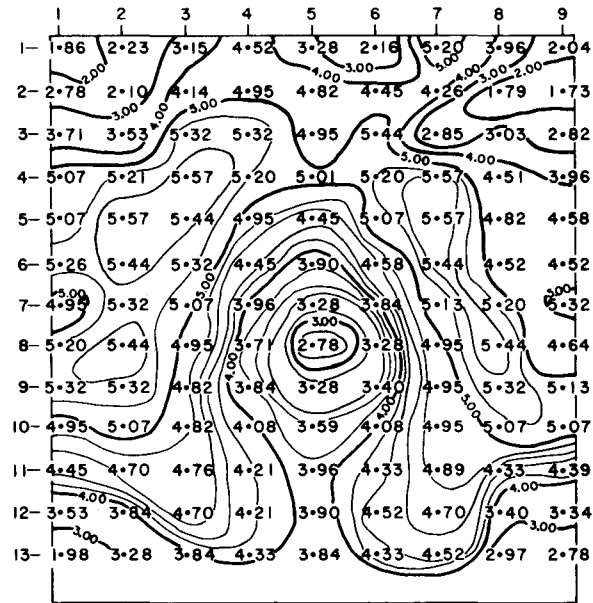
$$\bar{V}_r = \frac{Q}{A_r} \quad (5)$$



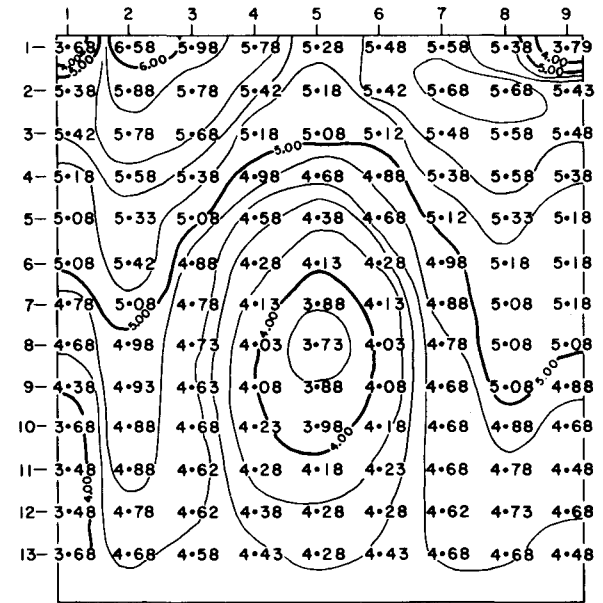
INTAKE NO. 1 - $\bar{V} = 2.837 \text{ m/s}$



INTAKE NO. 2 - $\bar{V} = 3.363 \text{ m/s}$



INTAKE NO. 3 - $\bar{V} = 4.288 \text{ m/s}$



INTAKE NO. 4 - $\bar{V} = 4.552 \text{ m/s}$

Figure 10.—Velocity distributions for the four intakes ($\theta=30^\circ$).

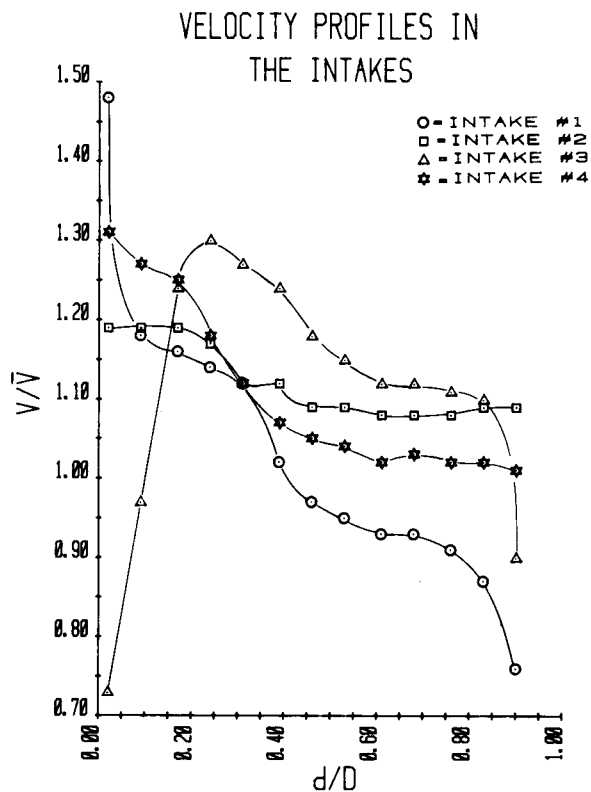


Figure 11.—Velocity profiles (top to bottom of intake) along data column 3 in figure 10.

The flow area at the runner was:

$$A_r = 0.6535 (D1)^2 \quad (6)$$

where $D1$ = the runner diameter

The data in table 1 can be used to compare relative losses between different geometries.

From equation (2),

$$\Delta p = \frac{\rho V^2}{E}$$

and in terms of head,

$$\frac{\Delta p}{\gamma} = \frac{V^2}{gE}$$

Thus, the relative loss between two configurations for equivalent discharges is:

$$\Delta h = \frac{\Delta p_2}{\gamma} - \frac{\Delta p_1}{\gamma} = \frac{V^2}{g} \left(\frac{1}{E_2} - \frac{1}{E_1} \right) \quad (7)$$

Equation 7 shows that the relative losses are proportional to velocity head. Therefore, actual losses will be more for higher discharges, if the Euler number is the same.

Example calculation of relative losses. — For a hypothetical prototype installation the following values are given:

Runner diameter — $D1 = 3.51$ m

Area at the runner — $A_r = 8.03$ m²

Gross prototype head — $H = 13.52$ m

Discharge relationship—

at $\theta = 0^\circ$, $Q = 127$ m³/s

at $\theta = 15^\circ$, $Q = 85$ m³/s

at $\theta = 30^\circ$, $Q = 43$ m³/s

Since $V_r = Q/A_r$ (equation 5),

at $\theta = 0^\circ$, $V_r = 15.82$ m/s

at $\theta = 15^\circ$, $V_r = 10.58$ m/s

at $\theta = 30^\circ$, $V_r = 5.36$ m/s

The Euler numbers in table 1 can be used to compute the relative head losses—using equation (7). Table 2 gives relative head losses for this example using intake 1 as a reference.

Table 2 shows that, for this example, intake 1 has about 1.5 percent less loss than the other intakes when the wicket gates are fully open ($\theta = 0^\circ$). However, when the gates are partially closed ($\theta = 15^\circ, 30^\circ$), intake 4 has less loss than intake 1. Intake 2 has less loss at $\theta = 30^\circ$. This is consistent with the velocity comparisons (figs. 10 and 11) showing that intakes 2 and 4 have a more uniform velocity distribution than intake 1.

Pressure drop coefficients. — Another form of the Euler number is the pressure drop coefficient,

Table 1. — Pressure drop through the model (Euler numbers)

Model with: draft tube / approach channel / bottom / no sides										
Wicket gate angle (degrees)	Intake 1		Intake 2		Intake 3		Intake 4		Intake 1 with pier	
	<i>E</i>	Run No.	<i>E</i>	Run No.						
0	4.321	149	4.178	166	4.195	186	4.173	197	4.121	140
15	3.535	150	3.425	167	3.435	187	3.559	198	3.549	141
20	2.360	162	2.349	171	—	—	—	—	2.407	145
25	1.728	163	1.754	172	—	—	—	—	1.748	146
30	1.297	151	1.322	168	1.290	188	1.340	199	1.258	142
35	.925	164	.967	173	—	—	—	—	.941	147
40	.683	165	.709	174	—	—	—	—	.674	148
45	.499	152	.500	169	.506	189	.491	200	.499	143
60	.153	153	.168	170	—	—	.158	201	.161	144

Intake 1 without draft tube										
Wicket gate angle (degrees)	With approach channel								With bulkhead slot and both sides	
	With both sides		With both sides (lowered)		With one side		With bottom and no sides		<i>E</i>	Run No.
	<i>E</i>	Run No.	<i>E</i>	Run No.	<i>E</i>	Run No.	<i>E</i>	Run No.		
0	1.810	120	1.813	129	1.814	134	1.821	137	1.808	101-104
15	1.648	121	1.650	130	1.644	135	1.650	138	1.662	105-107
20	1.465	125	—	—	—	—	—	—	—	—
25	1.210	126	—	—	—	—	—	—	—	—
30	.984	122	.985	131	.997	136	.975	139	1.000	108-110
35	.768	127	—	—	—	—	—	—	—	—
40	.567	128	—	—	—	—	—	—	—	—
45	.411	123	.413	132	—	—	—	—	.399	117-119
60	.143	124	.140	133	—	—	—	—	.145	115-116

Model with draft tube						
Wicket gate angle (degrees)	Intake 3					
	No approach channel		With approach channel and both sides		Intake 4 with no approach channel	
	<i>E</i>	Run No.	<i>E</i>	Run No.	<i>E</i>	Run No.
0	4.137	175	4.227	180	3.925	192
15	3.709	176	3.389	181	3.509	193
30	1.384	177	1.278	182	1.015	194
45	.519	178	.551	183	.380	195
60	.163	179	.164	184-185	.178	196

**E* = Euler number
 $E = \rho V^2 / \Delta p$; where ρ = density; V = velocity at the runner; Δp = pressure drop through the model (plenum pressure minus atmospheric pressure)

Table 2. — Comparison of intake losses

	$\theta = 0^\circ$		$\theta = 15^\circ$		$\theta = 30^\circ$	
	Δh (m)	$\Delta h/H$ (%)	Δh (m)	$\Delta h/H$ (%)	Δh (m)	$\Delta h/H$ (%)
Intake 2	0.202	1.5	0.104	0.8	-0.043	-0.3
Intake 3	.178	1.3	.094	.7	.012	.1
Intake 4	.210	1.6	-.022	-.2	-.073	-.5

θ = wicket gate angle (0° = fully open)
 Δh = difference in head loss from intake 1 (relative loss)
 H = gross head = 13.52 m

C_p . The pressure drop coefficient is the ratio of drop in pressure head to a reference velocity head (equation 8).

$$\text{Pressure drop coefficient} = C_p = \frac{\left(\frac{\Delta p}{\gamma}\right)}{\left(\frac{V^2}{2g}\right)} \quad (8)$$

where g = gravitational acceleration
 γ = specific force = ρg

It can be shown by combining equations (2) and (8) that:

$$C_p = \frac{2}{E}$$

and equation (7) becomes

$$\Delta h = \frac{V^2}{2g} (C_{p2} - C_{p1}) \quad (9)$$

Plotting C_p allows observation of losses in terms of a reference velocity head. Figure 12 is a comparison of pressure drop coefficients for the four intakes. The head required to move the flow through the model (for $\theta = 0^\circ$) is about 48 percent of the velocity head at the runner ($C_p = 0.48$). The plot illustrates the relative importance of intake losses to the overall losses. Intake 3, with no entrance curves, has the highest losses. However, even with no attempt to streamline the entrance, the losses in intake 3 are not significantly higher than in the other intakes. Intakes 2 and 4, with simplified and shortened entrances, show lower losses for partial gate openings than the traditional bellmouth-type design (intake 1), and they have a more uniform velocity distribution.

Additional testing. — Extensive testing of intake 1 was performed to determine the effect of other geometric features, including:

- A bulkhead slot
- A center pier in the intake
- The approach channel configuration
- A draft tube

Figure 13 shows intake 1 with a center pier and the approach channel with a bottom and no sides. Figures 14 through 17 illustrate the effect of these geometric features. Figure 14 is a comparison plot showing that the bulkhead slot has essentially no effect on losses. This figure also

illustrates the repeatability of the data. A pier in the intake (fig. 15) and the configuration of the approach channel leading to the intake (fig. 16) have little effect on the overall losses. However, the approach channel did have a significant effect in one case: The Euler numbers for intake 4 without an approach channel are lower than intake 4 with an approach channel bottom, except for $\theta = 60^\circ$. (See table 1, runs No. 192-196 vs. 197-201.) Tests on intake 1 did not show a significant effect due to the approach channel (runs No. 101-139). This difference can be explained by referring to figure 11. The relative velocity at the bottom of intake 1 is very low compared to intake 4. Therefore, the approach channel (which guides the flow into the bottom of the intake, preventing flow separation along the bottom) would be more important in intake 4 than in intake 1.

PRESSURE DROP THROUGH THE MODEL

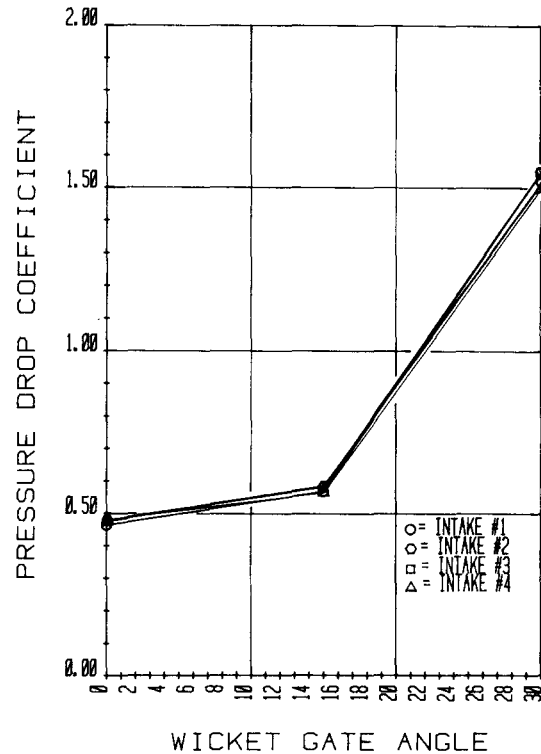


Figure 12.—Pressure drop through the model—comparison of four intakes.

Although the draft tube does not affect intake losses, tests were run with and without a draft

tube to determine the relative importance of the draft tube to the overall losses. The draft tube recovered about 60 percent of the runner velocity head (fig. 17). Losses through the model with the draft tube were less than one-half of the losses without the draft tube (at $\theta = 0^\circ$).

The wicket gate position has a significant effect on losses: C_p increases with decreasing gate opening (fig. 14). However, as the wicket gates are closed, the discharge decreases, thus reducing the actual magnitude of the head loss; because head loss is proportional to the velocity head (equation 7). Therefore, the gate opening vs. discharge relationship is needed to determine actual losses.

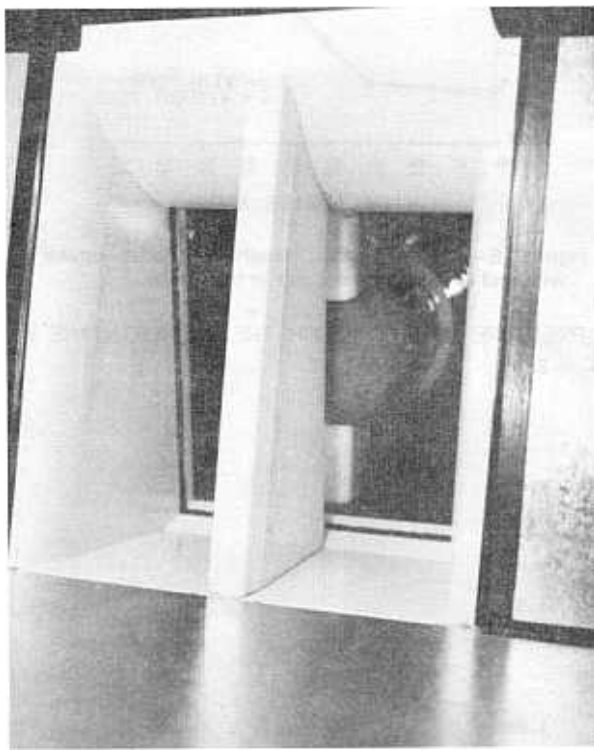


Figure 13.—Intake 1 with a center pier. Approach channel with bottom, no sides. P801-D-79888

Pressure drop along intake surfaces.—Pressures were measured along the top, bottom, and sides of each intake. Figures 18 through 21 show pressure drops along the surfaces for the four intakes. The reference velocity head in C_p for these plots is the average intake velocity head — $(V_j^2/2g)$, where $V_j = V_r/7.026$. For a typical

prototype situation the intake velocity head is about 1 percent of the gross head.

The reference distance ($L/D1$) is the distance from the front face of the intake to the piezometer (fig. 2).

The average pressure at the end of the intake section is an indication of the losses to that point. The average pressure drop coefficients at the end of the intakes were $C_{p1} = 1.216$, $C_{p2} = 1.200$, $C_{p3} = 1.497$, and $C_{p4} = 1.183$, for intakes 1, 2, 3, and 4 (from figs. 18 through 21). After subtracting the velocity head from the pressure drops, the energy losses—in terms of intake velocity heads—were 0.216, 0.200, 0.497, and 0.183 for intakes 1 through 4, respectively. This indicates that intake 3 has more than twice as much loss as the others and intake 4 has the lowest losses. It should be noted that the intake velocity head is only 2 percent of the runner velocity head. This puts the intake losses in perspective with the overall losses discussed previously.

Figures 22 through 25 compare pressures along the same surface for the four intakes. These figures illustrate that intake 3 has the highest local pressure drops, and intake 4 brings the pressure drop down in about one-half the distance of the other intakes, without high local pressure drops.

Intake pressure data accuracy.— The intake section pressures shown on figures 12 and 14 through 25 are average pressures. Figure 26 shows pressures recorded during one test, illustrating a typical range of pressure fluctuations for intake 1. Figure 27 shows the average pressures for three separate tests with similar conditions (see table 1 for test conditions). This figure illustrates the repeatability of the average pressure data in the intake section.

Wicket Gate Angle vs. Percent Gate Opening

Figure 28 is a cross reference for wicket gate angle, θ , vs. percent gate opening, where percent gate opening is defined as: open area/open area when gates are fully open. This figure should be useful in computing losses when the discharge relationship is given in terms of percent gate opening. If percent gate opening is defined as percentage of the full range of θ , the gate opening (in percent) is $(1-\theta/75) 100$.

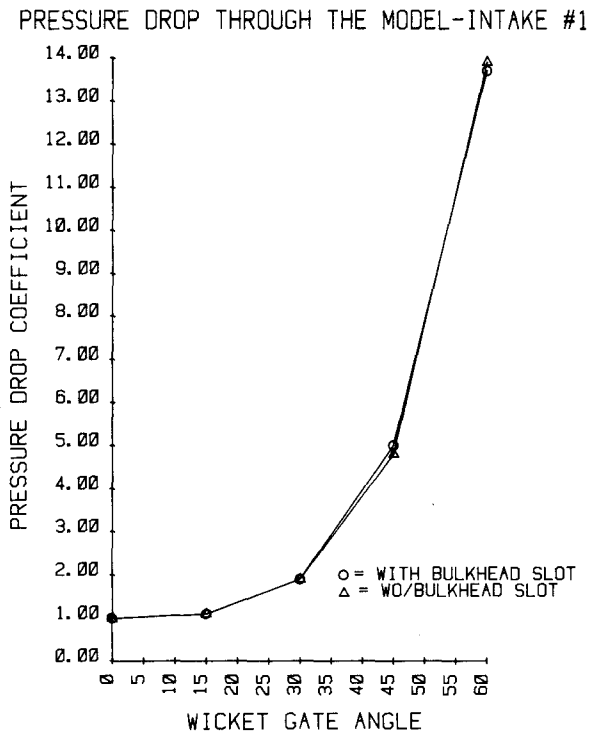


Figure 14.—Pressure drop through the model—intake 1, with and without a bulkhead slot.

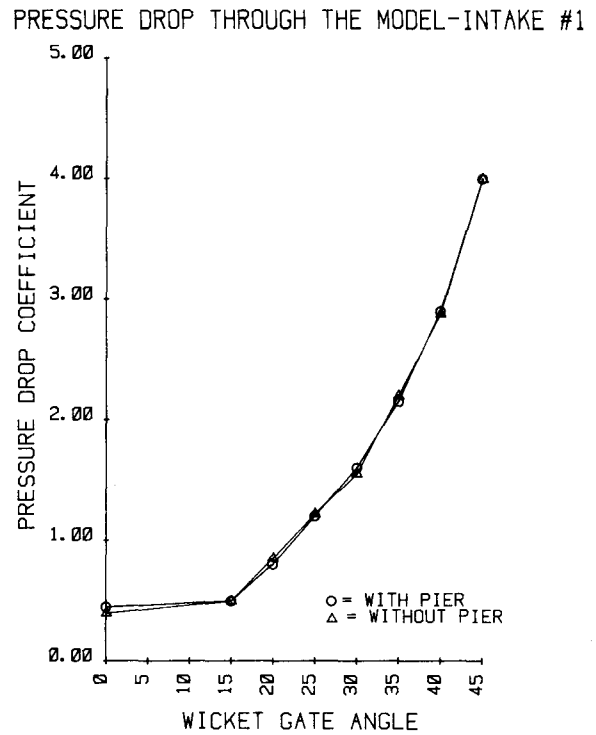


Figure 15.—Pressure drop through the model—intake 1, with and without a center pier in the intake.

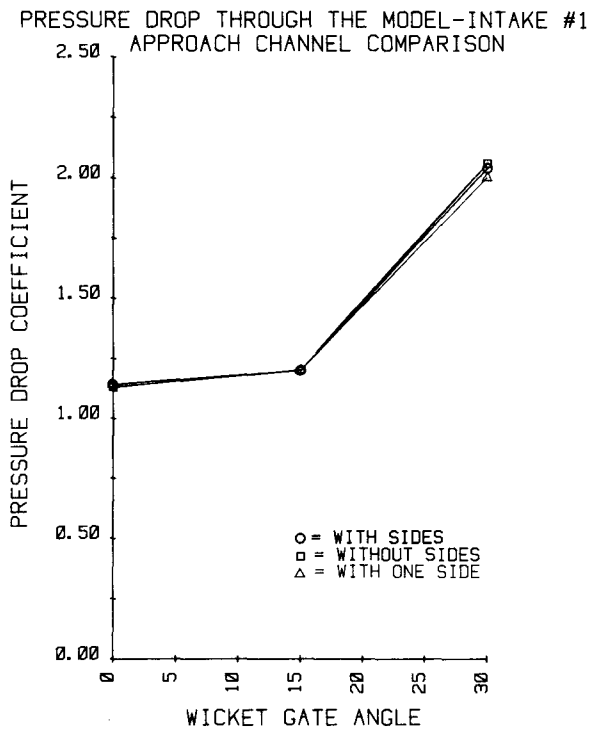


Figure 16.—Pressure drop through the model—intake 1, approach channel comparison.

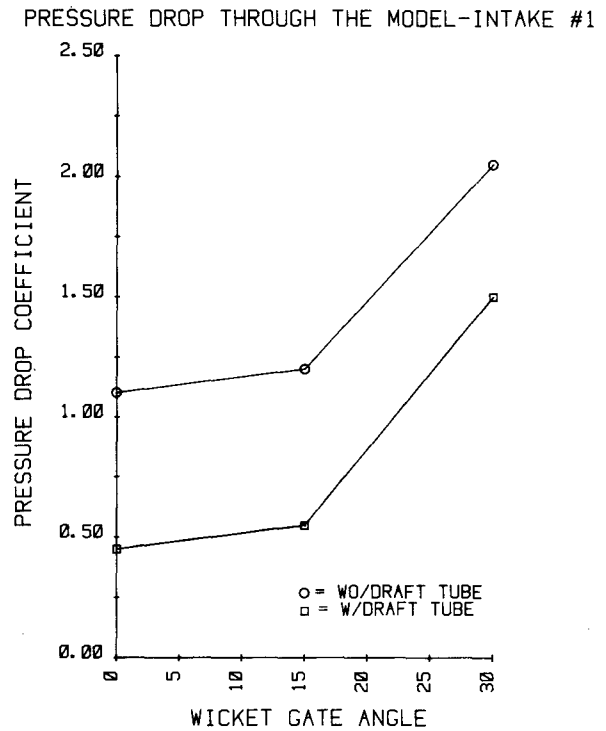


Figure 17.—Pressure drop through the model—intake 1, with and without a draft tube.

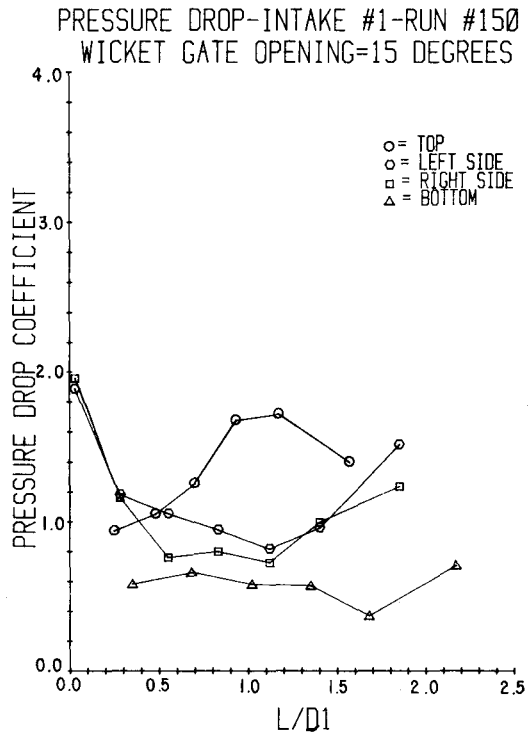


Figure 18.—Pressure drop along intake surfaces—intake 1.

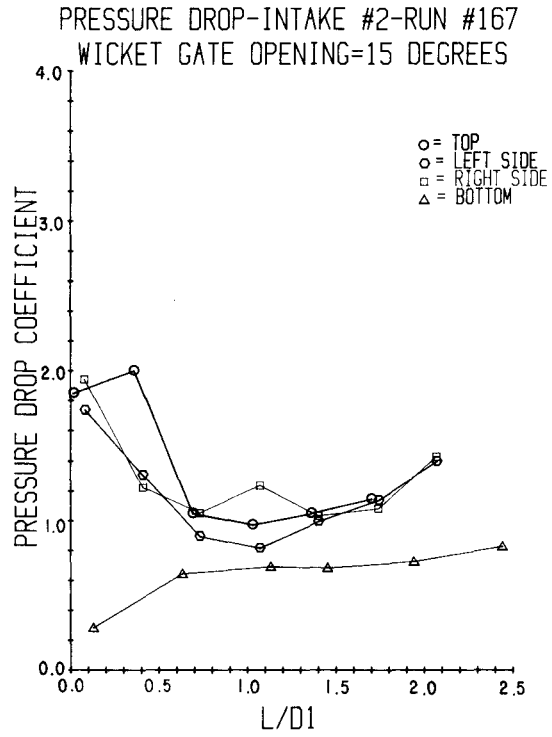


Figure 19.—Pressure drop along intake surfaces—intake 2.

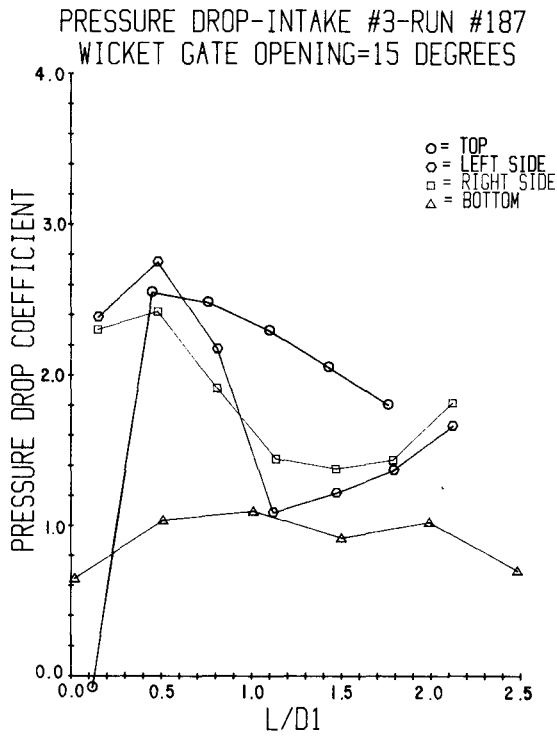


Figure 20.—Pressure drop along intake surfaces—intake 3.

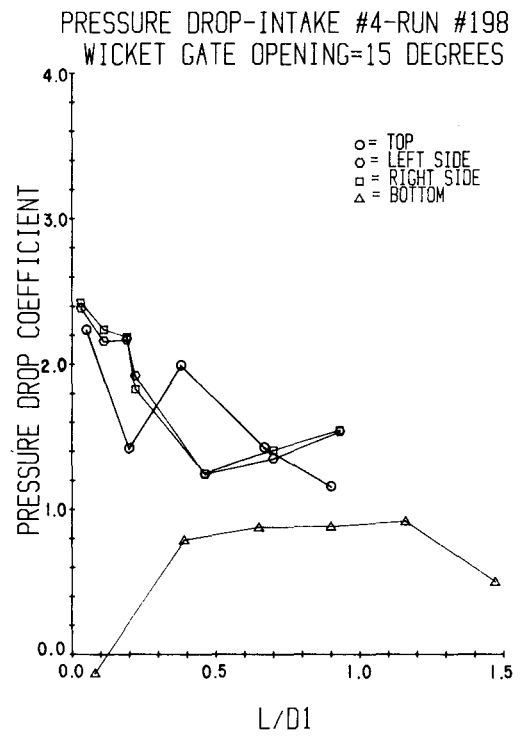


Figure 21.—Pressure drop along intake surfaces—intake 4.

PRESSURE DROP COMPARISON TOP CENTERLINE
WICKET GATE OPENING=15 DEGREES

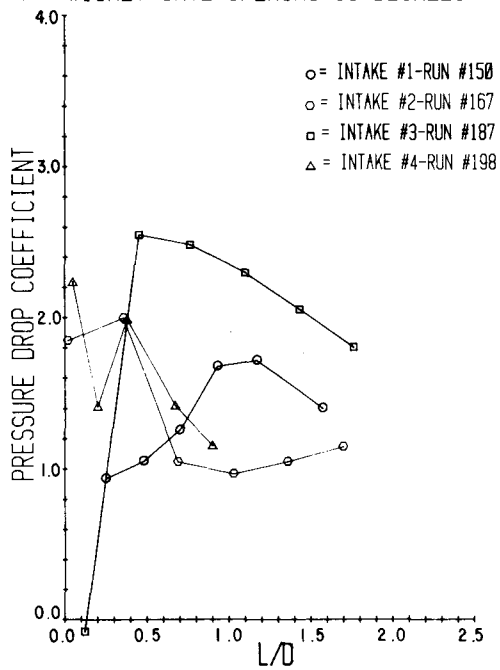


Figure 22.—Pressure drop comparison, top centerline—four intakes.

PRESSURE DROP COMPARISON LEFT SIDE CENTERLINE
WICKET GATE OPENING=15 DEGREES

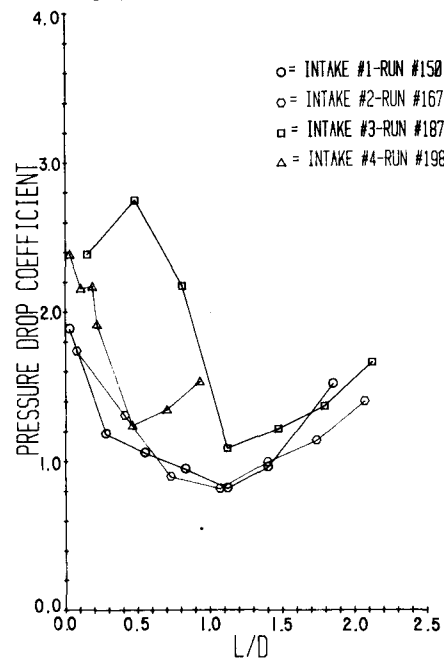


Figure 23.—Pressure drop comparison, left side centerline—four intakes.

PRESSURE DROP COMPARISON RIGHT SIDE CENTERLINE
WICKET GATE OPENING=15 DEGREES

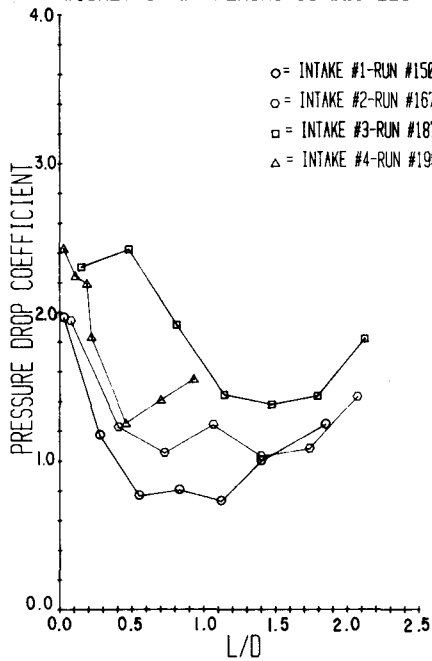


Figure 24.—Pressure drop comparison, right side centerline—four intakes.

PRESSURE DROP COMPARISON BOTTOM CENTERLINE
WICKET GATE OPENING=15 DEGREES

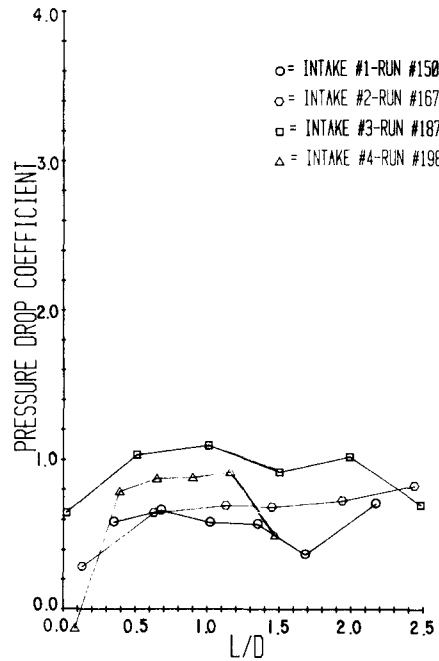


Figure 25.—Pressure drop comparison, bottom centerline—four intakes.

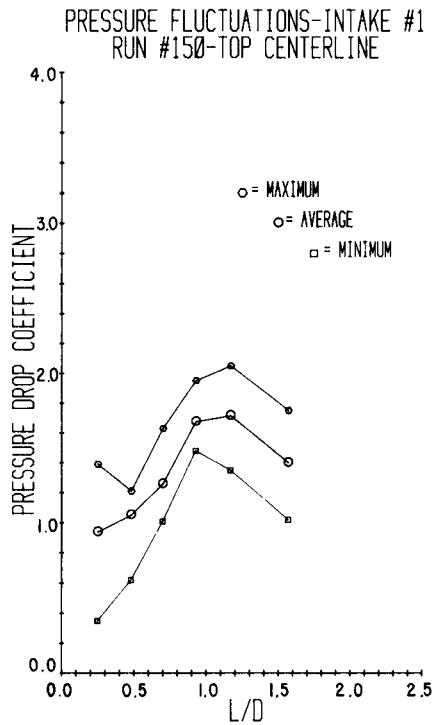


Figure 26.—Pressure fluctuations, intake 1, top centerline.

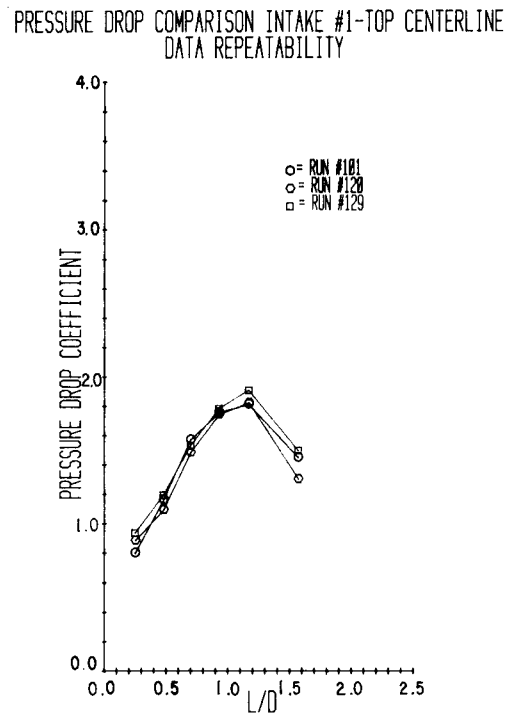


Figure 27.—Pressure drop comparison, intake 1, data repeatability.

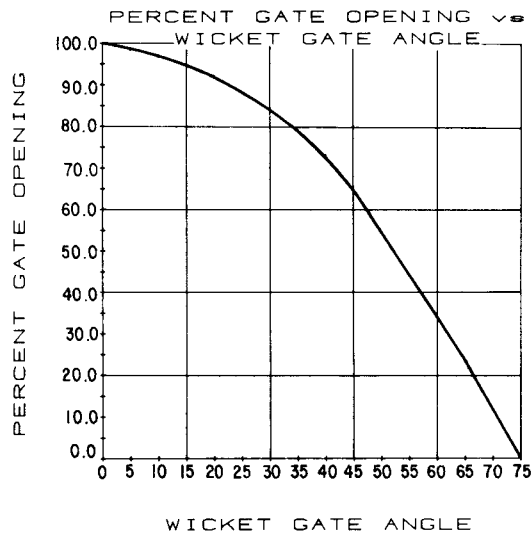


Figure 28.—Percent gate opening vs. wicket gate angle.

BIBLIOGRAPHY

- [1] Pugh, Clifford A., Bureau of Reclamation, "Intakes and Outlets for Low-Head Hydropower," *Journal of the Hydraulics Division*, ASCE, vol. 107, No. HY9, Proc. Paper 16494, pp. 1029-1045, September 1981.
- [2] Strohmer, Franz, Voest-Alpine, "Standardized Runners and Test Results Can Save Small Hydro Costs," *World Water*, pp. 43-48, November 1981.
- [3] Kobus, Helmut, *Hydraulic Modeling*, German Association for Water Resources and Land Improvement, Bulletin 7, pp. 5-6, pp. 288-289, 1978.
- [4] American Society of Mechanical Engineers, *Fluid Meters, Their Theory and Application*, 6th ed., ASME Research Committee on Fluid Meters, 1971.

Mission of the Bureau of Reclamation

The Bureau of Reclamation of the U.S. Department of the Interior is responsible for the development and conservation of the Nation's water resources in the Western United States.

The Bureau's original purpose "to provide for the reclamation of arid and semiarid lands in the West" today covers a wide range of interrelated functions. These include providing municipal and industrial water supplies; hydroelectric power generation; irrigation water for agriculture; water quality improvement; flood control; river navigation; river regulation and control; fish and wildlife enhancement; outdoor recreation; and research on water-related design, construction, materials, atmospheric management, and wind and solar power.

Bureau programs most frequently are the result of close cooperation with the U.S. Congress, other Federal agencies, States, local governments, academic institutions, water-user organizations, and other concerned groups.

A free pamphlet is available from the Bureau entitled "Publications for Sale." It describes some of the technical publications currently available, their cost, and how to order them. The pamphlet can be obtained upon request from the Bureau of Reclamation, Attn D-922, P O Box 25007, Denver Federal Center, Denver CO 80225-0007.